Synthesis and reactivity of functionalized cycloheptatrienyl–cyclopentadienyl sandwich complexes

Matthias Tamm

Received (in Cambridge, UK) 11th February 2008, Accepted 20th March 2008
First published as an Advance Article on the web 29th May 2008
DOI: 10.1039/b802289e

This *feature article* provides an overview of the synthesis and reactivity of functionalized cycloheptatrienyl–cyclopentadienyl transition metal sandwich complexes of the type $[(\eta^7\text{-}C_7H_7)M(\eta^5\text{-}C_5H_5)]$ (M = group 4, 5 or 6 metal), which can be used as building blocks for the preparation of metallopolymers and polymetallic complexes. Emphasis is placed on 16-electron group 4 complexes (M = Ti, Zr, Hf) and their reactivity towards σ-donor/π-acceptor ligands, which indicates that these complexes bear a close resemblance to Lewis acidic M^{+IV} complexes. Based on theoretical calculations, this behavior can be mainly attributed to the strong and appreciably covalent metal–cycloheptatrienyl interaction with the cycloheptatrienyl ring acting more as a −3 ligand than as a +1 ligand in these mixed ring complexes.

Introduction

Since the serendipitous synthesis and discovery of ferrocene,[1] its functionalization has become an important task in organometallic chemistry, and ferrocene-containing compounds are nowadays ubiquitous and indispensable to the development of research areas such as homogeneous catalysis and materials science.[2,3] In stark contrast, the modification of other sandwich complexes is significantly less developed, and for instance, little use has been made of sandwich complexes containing cycloheptatrienyl (Cht) ligands, although mixed cycloheptatrienyl–cyclopentadienyl (Cht–Cp) complexes of the type $[(\eta^7\text{-}C_7H_7)M(\eta^5\text{-}C_5H_5)]$ (M = group 4, 5 or 6 metal) have been known for more than three decades.[4] The mono- and diphosphanes $[(\eta^7\text{-}C_7H_6PR_2)Ti(\eta^5\text{-}C_5H_5)]$ and $[(\eta^7\text{-}C_7H_6PR_2)Ti(\eta^5\text{-}C_5H_4PR_2)]$ (R = Me, Ph) are among the very few examples of functionalized Cht–Cp complexes, and they have been obtained by mono- or dilithiation of $[(\eta^7\text{-}C_7H_7)Ti(\eta^5\text{-}C_5H_5)]$ (troticene) followed by reaction with the respective chlorophosphane $ClPR_2$.[5,6] In a similar fashion, a number of functionalized 17-electron vanadium complexes have been obtained from $[(\eta^7\text{-}C_7H_7)V(\eta^5\text{-}C_5H_5)]$ (trovacene) and used to study the intermetallic communication (exchange coupling) between the resulting paramagnetic sandwich moieties.[7]

Only recently, the interest in early-transition metal Cht–Cp complexes has become revitalized by independent reports from the groups of Elschenbroich, Braunschweig and Tamm on the preparation of *ansa*-Cht–Cp complexes (Fig. 1), which could be obtained from the 16-, 17- and 18-electron sandwich compounds $[(\eta^7\text{-}C_7H_7)M(\eta^5\text{-}C_5H_5)]$ (M = Ti, V, Cr).[8–10] It is the scope of this review to summarize the latest progress in this area, which has led to a number of new functionalized Cht–Cp sandwich complexes, and to demonstrate that there are in fact signs of life beyond ferrocene and other conventional metallocenes, if it comes to applications in materials science and homogeneous catalysis. Since the research contributed to this field from the author's group comprises mostly group 4 sandwich complexes, this article has its focus on the use of 16-electron Cht–Cp complexes containing the metals titanium, zirconium and hafnium.

Institut für Anorganische und Analytische Chemie, Technische Universität Carolo-Wilhelmina zu Braunschweig, Hagenring 30, 38106 Braunschweig, Germany. E-mail: m.tamm@tu-bs.de; Fax: +49 (531) 391-5387; Tel: +49 (531) 391-5309

Matthias Tamm was born in Berlin, Germany, in 1967 and studied chemistry at the Technische Universität Berlin, where he received his PhD in 1992 under the supervision of F. Ekkehardt Hahn. After spending one year as a Visiting Research Scientist at DuPont Central Research and Development, DE, USA with Anthony J. Arduengo, III, he returned to Germany in 1994 to complete his Habilitation in Berlin and Münster. Tamm was appointed to Privatdozent at the Westfälische Wilhelms-Universität Münster in 1999 and held a temporary professorship at the Technische Universität München from 2002 to 2005. He then moved to the Technische Universität Carolo-Wilhelmina zu Braunschweig in 2005 to become full professor of inorganic chemistry. His research interests lie in the areas of preparative organometallic chemistry and coordination chemistry with an emphasis on the development of novel, unusual ligand systems and on the application of their transition metal complexes in homogeneous catalysis, organic synthesis and materials science.

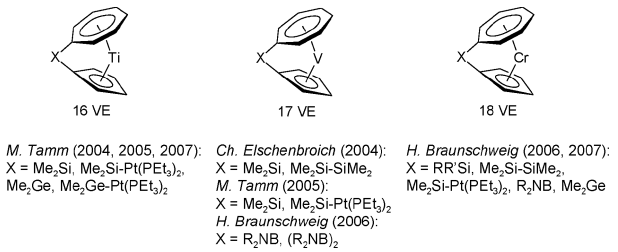

Fig. 1 *ansa*-Cycloheptatrienyl–cyclopentadienyl transition metal complexes.

Syntheses and electronic structures of group 4 cycloheptatrienyl–cyclopentadienyl sandwich complexes

The group 4 sandwich complexes $[(\eta^7\text{-}C_7H_7)M(\eta^5\text{-}C_5H_5)]$ (M = Ti, **1**; Zr, **2**; Hf, **3**) can be prepared in moderate yields by reduction of $[(\eta^5\text{-}C_5H_5)MCl_3]$ with magnesium in the presence of an excess of cycloheptatriene, C_7H_8 (Scheme 1).[11–13] After sublimation, the complexes are obtained as blue (**1**), purple (**2**) or orange-red crystalline solids (**3**), which have been characterized by means of X-ray diffraction analyses.[13–15] The three complexes, troticene (**1**), trozircene (**2**) and trohafcene (**3**),[16] are isostructural and crystallize in the orthorhombic space group *Pnma*. In each, the metal atom and one carbon atom in each ring reside on a crystallographic mirror plane. As these two carbon atoms adopt a *cis* orientation, the conformation of the two rings in **1**–**3** can be regarded as being perfectly eclipsed. The rings are virtually coplanar, and the centroid–metal–centroid angles are close to linearity (178.3° in **1**, 175.4° in **2**, 176.6° in **3**).

The bond lengths in **1**–**3** are summarized in Table 1. In all cases, the metal–carbon bonds to the seven-membered ring are significantly shorter than those to the five-membered ring, revealing a much stronger interaction between the metal centre and the cycloheptatrienyl ring (*vide infra*). The differences in the metal–centroid distances are significantly more pronounced, which can be mainly attributed to the larger diameter of the seven-membered ring, naturally allowing the larger ring to more closely approach the metal atom. Not surprisingly, substitution of titanium for zirconium and hafnium leads to considerably longer metal–carbon bond lengths, and also the shortening of the metal–carbon distances upon going from trozircene (**2**) to trohafcene (**3**) is in agreement with the trend of the metal radii.[17] Related structural features have also been observed for the closely related complexes $[(\eta^7\text{-}C_7H_7)M(\eta^5\text{-}C_5Me_5)]$ (M = Ti, Zr, Hf) containing the pentamethylcyclopentadienyl (Cp*) ligand.[18]

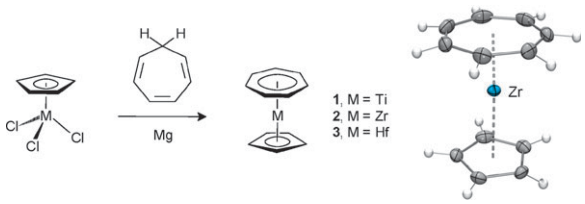

Scheme 1 Preparation of cycloheptatrienyl–cyclopentadienyl group 4 metal complexes and molecular structure of trozircene (**2**).

Table 1 Selected bond distances [Å] in complexes $[(\eta^7\text{-}C_7H_7)M(\eta^5\text{-}C_5H_5)]$ (M = Ti, Zr, Hf)

	M = Ti (**1**)	M = Zr (**2**)	M = Hf (**3**)
M–C_7	2.202(1)–2.2165(6)	2.323(2)–2.342(2)	2.293(3)–2.307(2)
M–C_7 (av.)	2.212	2.335	2.303
M–Ct_7[a]	1.487	1.664	1.612
M–C_5	2.3213(8)–2.3375(8)	2.494(2)–2.504(2)	2.457(3)–2.471(2)
M–C_5 (av.)	2.333	2.501	2.466
M–Ct_5[b]	1.988	2.195	2.151

[a] Ct_7 = centroid of the seven-membered ring. [b] Ct_5 = centroid of the five-membered ring.

The bonding of cycloheptatrienyl (η^7-C_7H_7) rings to early transition metals has been the subject of extensive experimental and theoretical investigation.[19–24] Originally, this ligand was regarded as a coordinated aromatic tropylium ion, $[\eta^7\text{-}C_7H_7]^+$, and thus classified as a six-electron donor with the assignment of a +1 formal charge in the resulting Cht metal complexes. The qualitative MO diagram in Fig. 2 is in agreement with this assignment, and the relative energies of the metal d orbitals and of the Cp and Cht e_1 and e_2 orbitals have been chosen such that the d orbitals are higher in energy than the filled ligand e_1 orbitals and lower in energy than the ligand e_2 orbitals, which remain empty if the ligands are both considered as six-electron ligands, *i.e.* as Cp^- and Cht^+, respectively. From the Frost–Musulin diagrams shown on the left, it can be easily deduced that both the e_1 and e_2 orbitals of the Cht ligand are lower in energy than those of the Cp ligand. Consequently, their relative energies with regard to the metal d orbitals indicate that the ligand-to-metal π-donation can be expected to be much more pronounced for the Cp ligand, whereas metal-to-ligand δ-back-donation represents the most significant contribution to metal–Cht binding. For 16-electron group 4 metal complexes, the resulting $1e_2$ orbitals are filled with four electrons and represent the highest occupied molecular orbitals (HOMOs), whereas the $1a_1$ orbital, which should be essentially metal d_{z^2} in character, represents the lowest unoccupied molecular orbital (LUMO). In contrast, this orbital contains one or two electrons in Cht–Cp complexes of group 5 (M = V, Nb, Ta) or group 6 (M = Cr, Mo, W) transition metals, respectively.

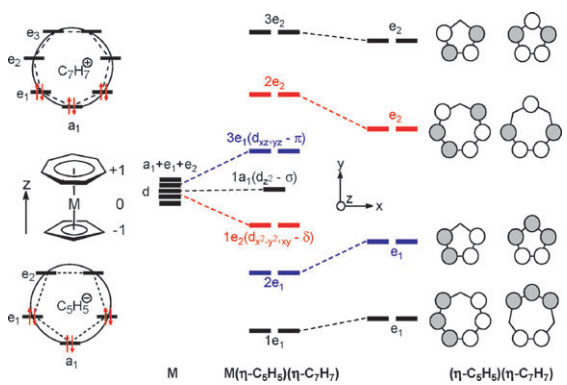

Fig. 2 Qualitative frontier molecular orbital diagram for $[(\eta^7\text{-}C_7H_7)M(\eta^5\text{-}C_5H_5)]$; the symmetry labels refer to the idealized point group $C_{\infty v}$, in which infinite axes of rotation are assumed for the carbocyclic rings.[23]

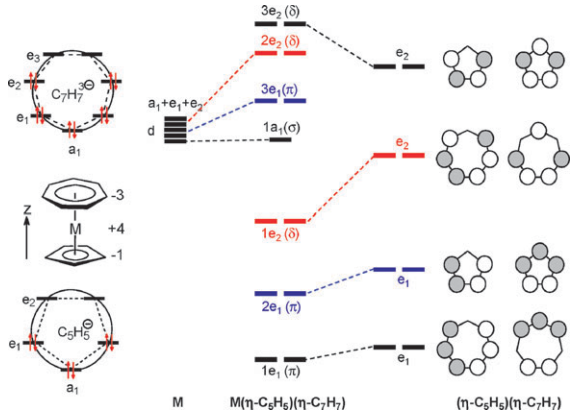

Fig. 3 Qualitative frontier molecular orbital diagram for $[(\eta^7\text{-}C_7H_7)M(\eta^5\text{-}C_5H_5)]$; the symmetry labels refer to the idealized point group $C_{\infty v}$, in which infinite axes of rotation are assumed for the carbocyclic rings.

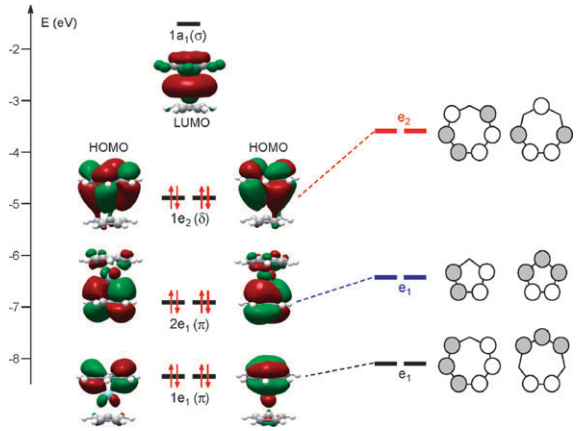

Fig. 4 Contour plots of the frontier orbitals in **2**.

Increase of the d orbital energies might eventually result in the bonding situation depicted in Fig. 3, where the Cht e_2 orbitals have become lower in energy than the metal d orbitals, so that the Cht–metal interaction must be formally regarded as ligand-to-metal δ-donation from a $[\eta^7\text{-}C_7H_7]^{3-}$ trianion, which would also satisfy the Hückel $4n + 2$ rule. Thereby, the ionic character of the Cp–metal π-interaction would become even pronounced. The decision, whether the MO diagram in Fig. 2 or that in Fig. 3 is better suited for such formal bonding considerations, can be derived from the relative metal d and Cht fragment contributions to the $1e_2$ frontier molecular orbitals. Table 2 summarizes the eigenvalues of the $1a_1$ (LUMO), $1e_2$ (HOMOs), $2e_1$ and $1e_1$ frontier orbitals in complexes **1**–**3** together with their metal, Cht and Cp fragment contributions.[25] For the HOMOs, the strong contributions from both the metal d and the Cht e_2 orbitals reveal a strongly covalent interaction with significant mixing of metal and ligand orbital character. Since the electrons in these orbitals are more ligand- than metal-localized, the bonding situation is in agreement with the representation in Fig. 3 and thus consistent with assigning a −3 formal charge to the C_7H_7 ligand. This situation becomes even more pronounced upon going from Ti (Cht/metal fragment contribution of 58/40%) to Zr (64/34%) and Hf (66/32%). The next two levels, the $2e_1$ and $1e_1$ orbitals, correspond to the π-interaction with the Cp and Cht rings, respectively, and their predominant ligand orbital character reveals only little mixing with the metal d orbitals. Accordingly, the interaction between the metal and the Cp ring, which lacks a δ-component, can be regarded as being mainly ionic. For the zirconium complex **2**, the contour plots of the relevant frontier molecular orbitals are given in Fig. 4, nicely illustrating the δ- and π-symmetry of the metal–ring interactions.

The $1a_1$ LUMO in complexes **1**–**3** is principally metal-localized and consists of the respective d_{z^2} orbital with small to marginal Cht and Cp contributions, in a coordinate system in which the metal–ring axis is defined as the z axis. The presence of an empty metal d orbital in each complex suggests that these systems should be susceptible to the addition of a two-electron donor ligand. However, the coordination of additional ligands to the titanium atom has never been observed for unbridged troticene (**1**), whereas the formation of thermally labile phosphane adducts had been previously reported for related zirconium and hafnium indenyl complexes of the type $[(\eta^7\text{-}C_7H_7)M(\eta^5\text{-}C_9H_7)]$. Only for M = Hf could a dinuclear complex containing a bridging 1,2-bis(dimethylphosphino)ethane (dmpe) ligand be structurally characterized.[26] This Lewis acidic behavior could be confirmed for trozircene (**2**), which forms isolable 1 : 1 complexes upon addition of alkyl and aryl isocyanides, 1,3,4,5-tetramethylimidazolin-2-

Table 2 Metal (M), Cht and Cp fragment contributions to the frontier orbitals in complexes $[(\eta^7\text{-}C_7H_7)M(\eta^5\text{-}C_5H_5)]$ (M = Ti, Zr, Hf)

Metal	Orbital	Symmetry[a]	Eigenvalue/eV	M (%)	Cht (%)	Cp (%)
Ti	49 (LUMO)	$1a_1$	−1.74	87	10	3
Zr			−1.58	90	7	3
Hf			−1.33	93	7	0
Ti	48, 47 (HOMOs)	$1e_2$	−4.99	40	58	2
Zr			−4.92	34	64	2
Hf			−4.86	32	66	2
Ti	46, 45	$2e_1$	−6.96	14	2	84
Zr			−6.93	9	6	85
Hf			−7.03	9	6	85
Ti	44, 43	$1e_1$	−8.31	10	89	1
Zr			−8.36	13	84	3
Hf			−8.33	12	85	3

[a] The symmetry labels refer to the idealized point group $C_{\infty v}$, in which infinite axes of rotation are assumed for the carbocyclic rings.

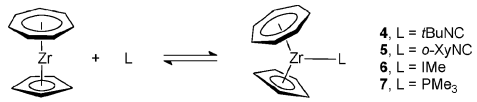

Scheme 2 Reaction of **2** with *tert*-butyl isocyanide (*t*BuNC), 2,6-dimethylphenyl isocyanide (*o*-XyNC), 1,3,4,5-tetramethylimidazolin-2-ylidene (IMe) and trimethylphosphine (PMe_3).

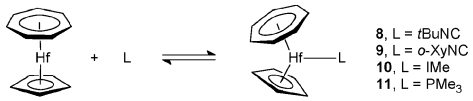

Scheme 3 Reaction of **3** with *tert*-butyl isocyanide (*t*BuNC), 2,6-dimethylphenyl isocyanide (*o*-XyNC), 1,3,4,5-tetramethylimidazolin-2-ylidene (IMe) and trimethylphosphine (PMe_3).

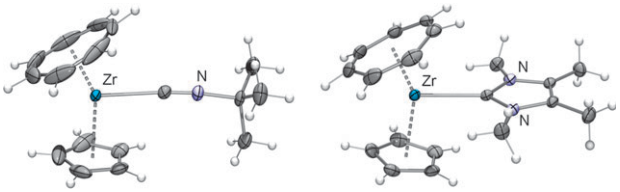

Fig. 5 Molecular structures of **4** (left) and **6** (right).

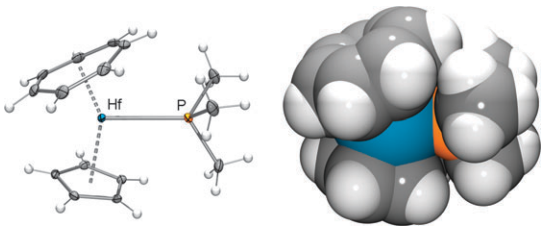

Fig. 6 Two presentations of the molecular structure of **11**.

ylidene (IMe) and trimethylphosphine (PMe_3) (Scheme 2).[15,27] The molecular structures of **4** and **6** are shown in Fig. 5. The isocyanide adducts **4** and **5** exhibit CN stretching vibrations at 2156 cm^{-1} (**4**) and 2134 cm^{-1} (**5**), which is only slightly shifted compared to the values for the free isocyanides. These observations indicate that metal-to-ligand π-back-bonding is weak and significantly less pronounced than in related zirconocene derivatives, in which the zirconium center is formally considered to be in the +II oxidation state. On the other hand, for d^0-configured Zr^{+IV} complexes, higher values, even above 2200 cm^{-1}, have been observed.[15]

Thermodynamic data for the reaction of **2** with *tert*-butyl isocyanide (*t*BuNC) could be established by means of an NMR titration study,[15] revealing that the reaction is only slightly exergonic with an average value of $\Delta G^\circ = -0.85 \pm 0.54$ kJ mol^{-1}. The average standard enthalpy for the formation of complex **4** and the associated entropy change amount to $\Delta H^\circ = -39.6 \pm 6.6$ kJ mol^{-1} and $\Delta S^\circ = -132.2 \pm 25.8$ J mol^{-1} K^{-1}, respectively, which clearly indicates a rather weak zirconium–isocyanide bond in comparison with conventional transition metal isocyanide complexes.[28] The experimental data are in excellent agreement with theoretical studies, and a calculated enthalpy of formation of $\Delta H^\circ = -36.5$ kJ mol^{-1} could be derived for **4**. The formation of the 2,6-dimethylphenyl isocyanide (*o*-XyNC) complex **5** is computed to be slightly more exothermic ($\Delta H^\circ = -38.2$ kJ mol^{-1}). *N*-Heterocyclic carbenes such as IMe are considered to be significantly stronger σ-donors than isocyanides, and accordingly, the calculated reaction enthalpy of formation of carbene complex **6** ($\Delta H^\circ = -56.3$ kJ mol^{-1}) suggests a stronger interaction, which could also be confirmed by NMR spectroscopy.[27] In contrast, the formation of the phosphane complex **7** is almost thermoneutral ($\Delta H^\circ = -2.3$ kJ mol^{-1}), which is also in accord with our inability to isolate this species from solution.[27]

The corresponding trohafcene complexes **8**–**11** containing *t*BuNC (**8**), *o*-XyNC (**9**), IMe (**10**) and PMe_3 (**11**) have been prepared only recently (Scheme 3),[13] and their molecular structures have been established by X-ray diffraction analyses. In contrast to the corresponding trozircene derivative **7**, the PMe_3 hafnium complex **11** could also be isolated in crystalline form and structurally characterized (Fig. 6). Table 3 summarizes the calculated enthalpies of formation of related trozircene and trohafcene complexes together with experimentally and theoretically derived metal–ligand distances. For each ligand, the formation of the hafnium complex is more exothermic than the formation of the corresponding zirconium complexes, and in agreement with the trend of the metal radii,[17] all Hf-ligand distances are shorter than the corresponding Zr–L distances. The Zr–C and Hf–C bond lengths in the isocyanide and carbene complexes **4**–**6** and **8**–**10** are comparable to those observed in Zr^{+IV} and Hf^{+IV} complexes, *e.g.* Zr–C = 2.313(3) Å and Hf–C = 2.275(4) Å in $[Cp_3M(CNtBu)]^+$ (M = Zr,[29] Hf[30]) and Zr–C = 2.432(3) Å and Hf–C = 2.401(2) Å in $[MCl_4L_2]$ (L = 1,3-diisopropylimidazolin-2-ylidene).[31] The experimentally observed Hf–P distance of 2.7851(5) Å in **11** is long, albeit significantly shorter than the calculated value of 2.90 Å (Table 3). The space filling presentation of its molecular structure reveals that steric interaction between the PMe_3 ligand and the Cht and Cp rings prevents strong metal–ligand interaction (Fig. 6), which is presumably the main reason for the exceptionally small calculated enthalpy of formation of −3.5 kJ mol^{-1}. Further experimental studies, *inter alia* by applying NMR titration techniques,[15] will be carried out to quantify and confirm the different stabilities of the Zr and Hf Cht–Cp complexes, since subtle differences in the reactivities of related zirconocene and

Table 3 Standard enthalpies for the formation of selected trozircene and trohafcene complexes; calculated and experimental metal–ligand distances

Complex	M	L	ΔH°_{calcd}/ kJ mol^{-1}	$d(M–L)_{calcd}$/Å	$d(M–L)_{exp}$/Å
4	Zr	*t*BuNC	−36.5	2.38	2.376(3)
8	Hf	*t*BuNC	−43.3	2.36	2.35[a]
5	Zr	*o*-XyNC	−38.2	2.36	—
9	Hf	*o*-XyNC	−46.0	2.32	2.306(2)
6	Zr	IMe	−56.3	2.51	2.445(2)
10	Hf	IMe	−63.1	2.47	2.393(2)
7	Zr	PMe_3	−2.3	2.94	—
11	Hf	PMe_3	−3.5	2.90	2.7851(5)

[a] Disordered structure, two independent molecules in the asymmetric unit.

hafnocene complexes have recently led to the isolation of remarkable organohafnium complexes and to "hafnium's foray into the limelight".[32,33]

Syntheses and reactivity of *ansa*-cycloheptatrienyl–cyclopentadienyl complexes

Double-lithiation of troticene (**1**) can be achieved with *n*-butyllithium–*N*,*N*,*N*′,*N*′-tetramethylethylenediamine (tmeda) resulting in the formation of the tmeda-stabilized complex [(η^7-C_7H_6Li)Ti(η^5-C_5H_4Li)].[6] The reaction of the dilithio complex with Me_2SiCl_2 or Me_2GeCl_2 afforded the sila- or germa[1]troticenophanes **12** and **13** as blue crystalline solids in moderate yield.[8a,c] The molecular structures of both complexes could be established by X-ray diffraction analyses, and Scheme 4 shows an ORTEP presentation of the germanium derivative **13**. Despite the considerable strain imposed by the introduction of the Me_2E-bridges (E = Si, Ge), the Cht and Cp rings in **12** and **13** are virtually planar and can still be regarded as being essentially η^7- or η^5-coordinated, respectively. The deviation from an unstrained sandwich structure with an ideal coplanar ring orientation, as observed in troticene,[14] can be characterized by the angles α, β, β', θ and δ, which are defined in Table 4. Since germanium has a larger covalent radius than silicon, one would expect the germa[1]-troticenophane **13** to be somewhat less distorted than the sila[1]troticenophane **12**, and this is confirmed by the observation of a slightly smaller tilt angle α (22.9° in **13** *versus* 24.1° in **12**). The same trend has been observed for other structurally characterized Si/Ge couples, the ferrocenophanes **14**/**15**,[34,35]

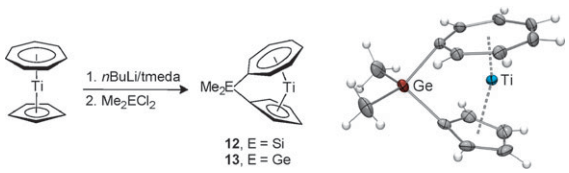

Scheme 4 Preparation of silicon- and germanium-bridged *ansa*-cycloheptatrienyl–cyclopentadienyl titanium complexes and molecular structure of **13**.

Table 4 Structural comparison of silylene- and germylene-bridged *ansa*-complexes

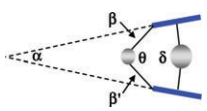

Compound	α/°	β/°, β'/°	θ/°	δ/°
12	24.1	42.3, 29.2	95.6	160.5
13	22.9	41.4, 28.5	92.8	161.0
14	20.8	37.0	95.7	164.7
15	19.1	37.8, 35.9	91.7	—
16	16.6	38.2, 37.9	92.9	167.6
17	14.4	38.7	91.8	—
18	17.3	48.3, 32.6	98.2	167.0
19	15.6	47.7, 30.6	93.9	168.4
20	15.1	43.8, 29.8	90.5	168.3

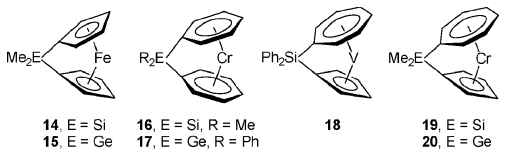

Fig. 7 Selected silylene- and germylene-bridged *ansa*-complexes.

the chromarenophanes **16**/**17**[36,37] and the trochrocenophanes **19**/**20**[10b,d] (Fig. 7, Table 4).

It can be clearly concluded that both **12** and **13** represent the most strongly distorted sandwich complexes in comparison to the silylene- and germylene-bridged derivatives shown in Fig. 7. For instance, a pronounced decrease in strain is observed on going from the 16-electron sila[1]troticenophane **12** (α = 24.1°, δ = 160.5°) to the 17-electron sila[1]trovacenophane **18** (α = 17.3°, δ = 167.0°)[9] and to the sila[1]trochrocenophane **19** (α = 15.6°, δ = 168.4°),[10b] which is undoubtedly a consequence of the larger interannular distance in [(η^7-C_7H_7)Ti(η^5-C_5H_5)] (troticene, 3.48 Å) compared to that in [(η^7-C_7H_7)V(η^5-C_5H_5)] (trovacene, 3.38 Å) and in [(η^7-C_7H_7)Cr(η^5-C_5H_5)] (trochrocene, 3.26 Å).[14a] Large angles β and β' are observed for **12** (42.3°, 29.2°) and **13** (41.4°, 28.5°), indicating a strong distortion from planarity at the *ipso*-carbon atoms (Table 4). These values are only exceeded by the corresponding angles found in the vanadium and chromium congeners **18** (48.3° and 32.6°), **19** (47.7° and 30.6°) and **20** (43.8° and 29.8°). This trend, however, must not necessarily impose higher strain on these sandwich molecules in comparison to **12**, since a significant out-of-plane displacement of the substituents of the Cht ring can also partially be attributed to a reorientation of the large seven-membered ring for a better overlap with the smaller vanadium and chromium atoms.[4,38]

As mentioned before, coordination of additional ligands has never been observed for troticene (**1**). However, bridging and bending of the two rings in **12** and **13** creates a gap at the titanium atom, which might thereby become accessible to "slender" monodentate ligands such as carbon monoxide and isocyanides. To identify suitable frontier orbitals for such metal–ligand interactions, the structure of the silicon-bridged troticenophane **12** was optimized with DFT methods.[8a] Owing to the distortion of the symmetric sandwich structure, the highest occupied molecular orbitals in **12** have given up their degeneracy. Their energy positions are nonetheless very close to those in **1**. A closer inspection (Fig. 8, Table 2) reveals that the introduction of the *ansa*-bridge leads to a slight increase in the HOMO–LUMO gap. Since the lowest energy band in the optical absorption spectrum of **1** has been assigned to a one-electron HOMO–LUMO transition, which is partly a d–d transition and partly a ligand-to-metal charge transfer (LMCT),[39] UV-Vis measurements could be used to quantify these effects: a blue shift of the lowest energy band in the visible spectrum with enhanced intensity owing to a lowering of the symmetry and as a consequence of relaxation of the Laporte selection rule was observed (from λ = 696 nm and ε = 31 L mol^{-1} cm^{-1} in **1** to λ = 663 nm and ε = 105 L mol^{-1} cm^{-1} in **12**). It is worth noting that the introduction of a Si bridge in troticene has an opposite effect on the splitting and

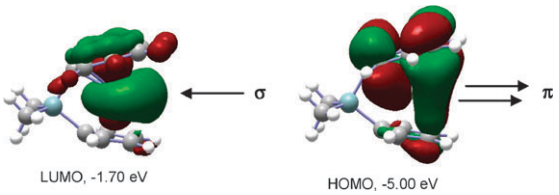

Fig. 8 Contour plots and eigenvalues of the frontier orbitals in **12**.

energy of the molecular orbitals than observed for sila[1]-ferrocenophanes and other [1]ferrocenophanes.[3g,40]

The electronic structure calculation of **12** reveals that this 16-electron complex contains a LUMO and a HOMO (Fig. 8) that seem to be suitably oriented for σ- and π-interaction with one additional ligand. However, the formation of a stable carbonyl complex of type **21** (Scheme 5) could not be detected at ambient pressure. An NMR spectroscopic study of **12** under elevated CO pressure in the temperature range from +20 to −70 °C indicates that the metal–CO interaction is very weak and that CO is quickly exchanged on the NMR time scale.[8a] An exchange to more σ-donating, less π-accepting isocyanide ligands produced the adducts **22** and **23** as brown crystalline solids in nearly quantitative yields (Scheme 5). As also observed for the trozircene–isocyanide complexes **4** and **5** (Scheme 2), the CN stretching vibrations at 2153 cm^{-1} (**22**) and at 2112 cm^{-1} (**23**) are only slightly shifted compared to the values of the free isocyanides, again indicating only weak metal-to-ligand π-back-donation. In principle, it should be possible to quantify the interaction between **12** and the CO and isocyanide ligands and to produce thermodynamic and kinetic data for these equilibrium reactions by employing NMR titration techniques as described for the trozircene-*tert*-butyl isocyanide adduct **4**.[15] Fig. 9 shows excerpts from the ^{1}H NMR spectra of **12** at 20 °C with variation of the isocyanide concentration. Upon increase of the isocyanide concentration, the resonances for the ring hydrogen atoms are clearly shifted, although in different directions and to a different extent, depending on their position on the rings. Monitoring the change of the chemical shifts as a function of the isocyanide concentration and application of an NMR adaptation[41] of the Benesi–Hildebrand treatment, originally used in optical spectroscopic studies,[42] allows the equilibrium constant K_C to be established for a given temperature. Determination of K_C at different temperatures produces ΔH° and ΔS° from a van't Hoff plot of ln K_C *versus* $1/T$. Unfortunately, the data for the formation of **22** do not seem to be fully reliable, since the almost thermoneutral nature of this reaction ($\Delta H^\circ = +6.7 \pm 3.4$ kJ mol^{-1}) leaves K_C hardly affected by variation of the temperature. Yet, it can be concluded that the interaction is actually very weak, which is also confirmed by the calculated enthalpy of formation of $\Delta H^\circ = -14.5$ kJ mol^{-1}.

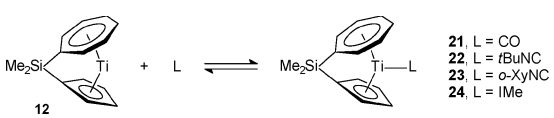

Scheme 5 Reaction of **12** with carbon monoxide (CO), *tert*-butyl isocyanide (*t*BuNC), 2,6-dimethylphenyl isocyanide (*o*-XyNC) and 1,3,4,5-tetramethylimidazolin-2-ylidene (IMe).

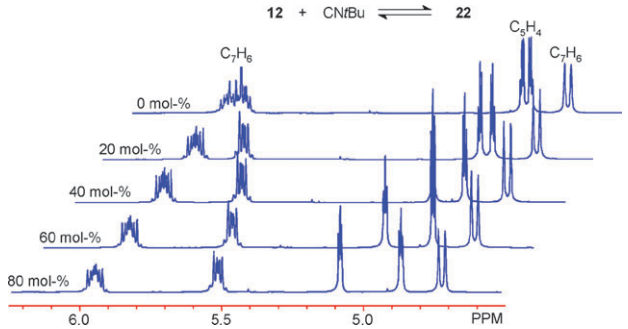

Fig. 9 Excerpts from the ^{1}H NMR titration of **12** with *t*BuNC in toluene-d_8 at 20 °C.

The molecular structures of **12** and its *t*BuNC adduct **22** are shown in Fig. 10. Coordination of the isocyanide ligand leads to pronounced elongation of the metal–carbon bonds, in particular to the seven-membered ring [from 2.170(3)–2.256(2) Å to 2.248(2)–2.412(3) Å]. Hence, the distance between titanium and the centroid of the seven-membered ring increases from 1.496 to 1.649 Å. As a result, modified coordination is observed in the solid state, indicating a distortion from a symmetric η^7- towards an open η^5-bonding mode.[43] In agreement with the small Ti–isocyanide bond dissociation energy (*vide supra*), the Ti–CN*t*Bu distance is long [2.223(2) Å] and falls in the range observed for Ti^{+IV} complexes, where the d^0-electron configuration prevents effective metal-to-ligand back-donation. Despite its weakness, however, π-interaction can be held responsible for the observation that the 2,6-dimethylphenyl isocyanide ligand in **23** adopts a vertical conformation with a coplanar orientation toward the mirror plane including titanium, silicon and the centroids of the Cht and Cp rings (Fig. 11). This orientation, which was also experimentally and theoretically confirmed for the corresponding trozircene *o*-XyNC complex **5**,[15] is electronically favorable, since it allows the alignment of the LUMO of the isocyanide ligand in an antisymmetric fashion with respect to the mirror plane in order to optimally interact with the HOMO of the troticenophane **12** (Fig. 8). In contrast, a horizontal conformation is observed for complex **24**, which contains an imidazolin-2-ylidene ligand with stronger σ-donor and weaker π-acceptor characteristics (Fig. 11). As expected, the calculated enthalpy of formation of $\Delta H^\circ = -27.8$ kJ mol^{-1} indicates a stronger metal–ligand interaction than in **22**.

In view of the similar reactivity of sila[1]troticenophane (**12**) and of trozircene (**2**) and trohafcene (**3**) towards carbon monoxide or isocyanides, it can be concluded that these 16-electron complexes have only a small propensity to efficiently interact with σ-donor/π-acceptor ligands. In this respect, **2**, **3** and **12** do not act like complexes containing titanium,

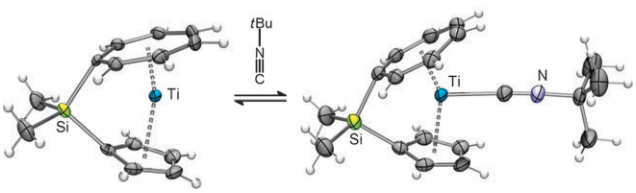

Fig. 10 Molecular structures of **12** and **22**.

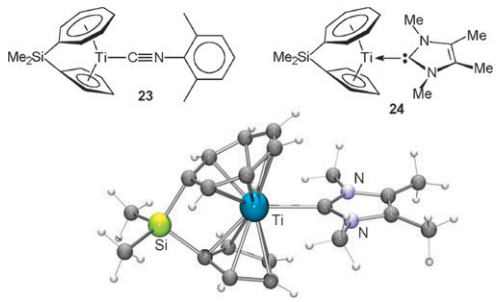

Fig. 11 Schematic presentation of the solid state conformations of **23** and **24** (top); molecular structure of **24** (below).

zirconium or hafnium in a lower oxidation state but rather bear a closer resemblance to Lewis acidic M^{+IV} complexes. Based on theoretical calculations, this behavior can be mainly attributed to the strong and appreciably covalent metal–cycloheptatrienyl interaction leading to highly stabilized frontier orbitals and consequently to a diminishing π–electron release capability. Therefore, these experimental results support the conclusion that the cycloheptatrienyl ring functions more as a −3 ligand than as a +1 ligand in these mixed ring complexes,[24] a description, which was also found to be valid for cycloheptatrienyl sandwich compounds of actinides.[44]

Ring-opening reactions of *ansa*-cycloheptatrienyl–cyclopentadienyl complexes

Poly(ferrocenes) represent the most important class of transition metal-containing macromolecules and are playing an important role in the development of novel polymers with intriguing structural, conductive, magnetic, optical, or redox properties.[3] In most cases, these polymers are made by ring-opening polymerization (ROP) of strained [1]ferrocenophanes such as **14** (Scheme 6), which can be initiated thermally or by anionic or transition metal catalysis. In contrast to the Cp–Si–Cp-linked poly(ferrocenylsilane) obtained from **14**, thermal ROP of the troticenophanes **12** and **13** apparently leads to irregular polymers, which contain all possible Cp–X–Cp, Cht–X–Cht and Cp–X–Cht (X = Me_2Si, Me_2Ge) linkages (Fig. 12).[8a,b] It could be demonstrated that **12** exothermically polymerizes at about 170 °C, whereas **13** ring-opens at lower temperature at about 130 °C. This different behavior can be attributed to the weaker germanium–carbon bond in **13** compared to the silicon–carbon bond in **12**. The strain energies of both molecules were estimated to be approximately 45 kJ mol^{-1} by means of differential scanning calorimetry (DSC) studies,[8c] and Fig. 12 shows the DSC trace of **12**.

Interestingly, the strain energies of **12** and **13** are substantially smaller than the values reported for related [1]ferrocenophanes, *e.g.* 80 kJ mol^{-1} for **14**,[45] although the structural

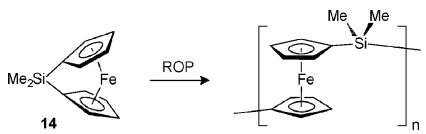

Scheme 6 Ring-opening polymerization of sila[1]ferrocenophane **14**.

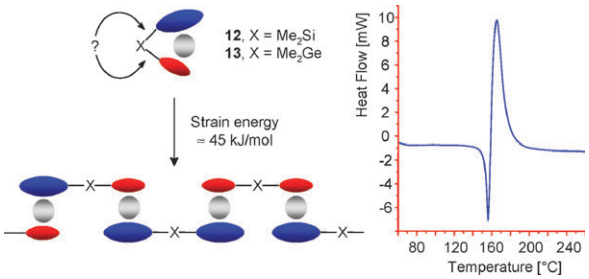

Fig. 12 Left: schematic presentation of the ring-opening polymerization of **12** and **13** (blue = Cht, red = Cp, grey = Ti); right: DSC thermogram of **12** with a melt endotherm at 155 °C and a polymerization exotherm at 170 °C.

parameters of **12** and **13** (Table 4) suggest that these molecules are more strongly distorted from an unstrained sandwich structure. An explanation could be derived from a theoretical comparison of the energy content of ferrocene (Cp_2Fe) and troticene (**1**) as a function of the bending angle δ (Fig. 13).[25] As expected, bending of both sandwich molecules results in an exponential increase of energy.[46] For ferrocene, however, a significantly steeper rise in energy is observed upon lowering δ, and it can be clearly deduced that distortion of the $[(\eta^5\text{-}C_5H_5)_2Fe]$ moiety requires significantly more energy than that of $[(\eta^7\text{-}C_7H_7)Ti(\eta^5\text{-}C_5H_5)]$. As a consequence, the energy released by conversion of a strained into an unstrained molecule is in fact expected to be higher for ferrocenophanes than for troticenophanes.

To elucidate the impact of the d-electron configuration on the strain energy, bending of the 17- and 18-electron species trovacene and trochrocene was also investigated theoretically (Fig. 13). Comparison with the calculations obtained for metallocenes (Cp_2M)[46] leads to the expectation that occupation of the $1a_1$ orbital (Fig. 4) with one (M = V) or two electrons (M = Cr) should more strongly favour parallel ring structures. Although this trend should be even further supported by decreasing the interannular distance in the order Ti > V > Cr (*vide supra*),[14a] the calculations do not show a definite pattern (Fig. 13). Whereas the energy penalty for bending trochrocene is expectedly higher in comparison to troticene and almost identical to that of its 18-electron congener ferrocene, the trovacene energies for a given angle δ are

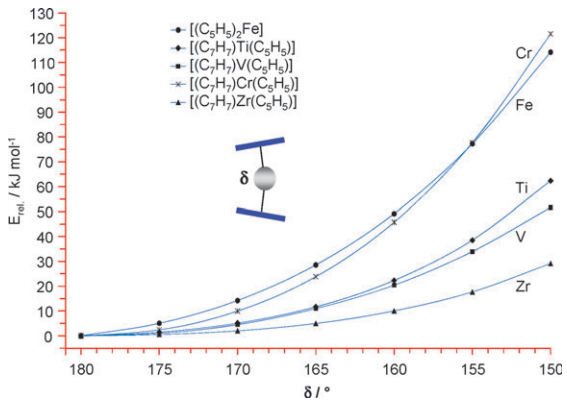

Fig. 13 Relative potential energy for ferrocene and troticene as a function of the angle δ.

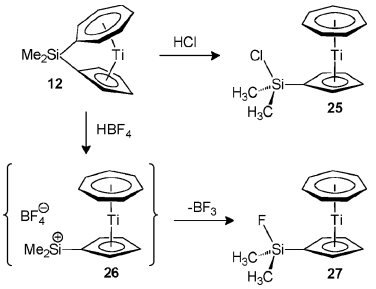

Scheme 7 Acid-induced ring-opening of **12**.

consistently smaller than those of troticene, indicating that simple parallels to bent metallocenes cannot be drawn.[46] The shallow potential calculated for the bending of trozircene (**2**) (Fig. 13), however, is in full agreement with the observed reactivity and ability of **2** to coordinate additional σ-donor ligands.

Since the thermal ring-opening polymerization of *ansa*-Cht–Cp complexes leads to the formation of irregular polymers (Fig. 12), the possibility of regioselective Si–C bond cleavage in **12** was investigated. Treatment of **12** with ethereal HCl exclusively affords the troticene derivative **25** with a chlorodimethylsilyl substituent attached to the Cp ring,[8c] indicating that a regioselective protonolysis of the silicon–carbon bond to the seven-membered ring must have occurred (Scheme 7). In a similar fashion, the reaction with ethereal HBF_4 produces the fluorosilane **27**, which presumably proceeds *via* a highly reactive silyl cation intermediate **26**, which is able to abstract F^- from the tetrafluoroborate anion. It should be noted that this mechanism had already previously been established for the same reaction employing sila[1]ferrocenophanes such as the dimethylsilyl-bridged derivative **14**.[47] The regioselective Si–C bond cleavage and exclusive protonation of the Cht ring could have been anticipated from the structural constraints in **12** (Table 4), where the unusually large β angle of 42.3° at the Si–C_7H_6 site implies that this Si–C bond or rather the *ipso*-C_7H_6 carbon atom represent the most highly strained part of this molecule.

Regioselective Si–C bond cleavage could also be observed on treatment of **12** with equivalent amounts of tris(triethylphosphane)platinum(0), which results in the formation of the platinasila[2]troticenophane **29** by oxidative addition and insertion of a $[Pt(PEt_3)_2]$ moiety into the Si–C bond to the seven-membered ring (Scheme 8).[8b,c] In a similar fashion, the analogous vanadium and chromium complexes **30** and **31** could be isolated from the respective sila[1]trovacenophane **28**[8b] and sila[1]trochrocenophane **19**.[10b] The molecular structures of **29**–**31** could be established by X-ray diffraction analyses, and Scheme 8 shows the structure of the Ti derivative **29**. All three compounds are isotypic and crystallize in the orthorhombic space group $P2_12_12_1$. Selected bond lengths and angles are summarized in Table 5. As expected from the crystal structures of the parent complexes $[(\eta^7\text{-}C_7H_7)M(\eta^5\text{-}C_5H_5)]$ (M = Ti, V, Cr),[14a] the metal–carbon bond distances decrease in the order Ti > V > Cr. Accordingly, **29** shows the strongest deviation from an unstrained sandwich structure with α = 13.5° and δ = 169.1°. Smaller angles α together with larger angles δ are consequently observed for the vanadium (α = 10.6°, δ = 171.9) and chromium analogues (α = 7.5°, δ = 174.9°). In all complexes, the platinum centres are in a slightly distorted square-planar environment with two different PEt_3 ligands. Because of the strong *trans* influence of the silyl substituents, the Pt–P1 distances are significantly longer than Pt–P2. These distances and also the Pt–C and Pt–Si bond lengths are in reasonable agreement with the values obtained from structural characterization of related platinasila[2]ferrocenophanes.[48] Finally, it should be noted that Pt insertion could also be observed for the germa[1]troticenophane **13**,

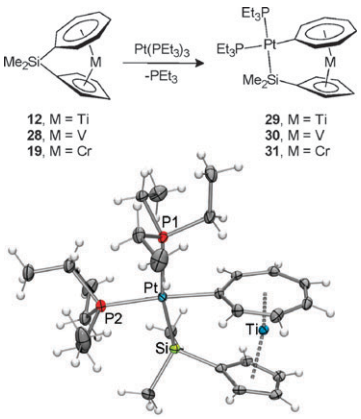

Scheme 8 Synthesis of Si–Pt-bridged *ansa*-Cht–Cp complexes and structure of **29**.

Table 5 Selected bond distances [Å] and angles [°] in complexes of the type $[(PEt_3)_2PtSiMe_2(\eta^7\text{-}C_7H_6)M(\eta^5\text{-}C_5H_4)]$

	M = Ti (**29**)	M = V (**30**)	M = Cr (**31**)
M–C_7	2.184(3)–2.216(3)	2.168(3)–2.192(3)	2.141(4)–2.173(4)
M–C_7 (av.)	2.203	2.184	2.149
M–Ct_7[a]	1.468	1.446	1.411
M–C_5	2.280(3)–2.333(3)	2.209(3)–2.274(3)	2.150(4)–2.201(4)
M–C_5 (av.)	2.308	2.242	2.174
M–Ct_5[b]	1.967	1.888	1.808
Pt–C	2.096(3)	2.092(2)	2.087(4)
Pt–P1	2.3874(6)	2.3849(6)	2.3745(10)
Pt–P2	2.2962(9)	2.3020(7)	2.3057(10)
Pt–Si	2.3881(8)	2.3900(6)	2.4229(13)
α	13.5	10.6	7.5
δ	169.1	171.9	174.9

[a] Ct_7 = centroid of the seven-membered ring. [b] Ct_5 = centroid of the five-membered ring.

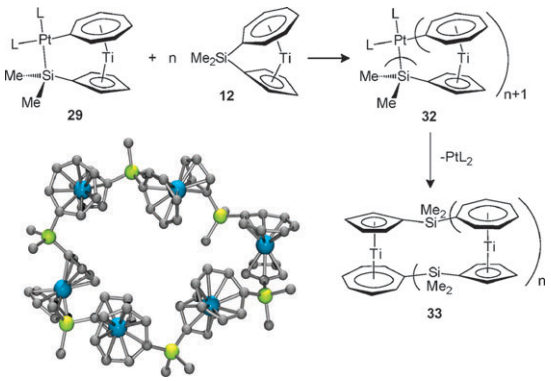

Scheme 9 Synthesis of oligo(troticenylsilanes); calculated structure of a cyclic hexamer **33** (n = 5).

resulting in the formation of a metallacycle with a rare Ge–Pt bond.[8c]

The Pt–Si-bridged derivative **29** could be used as a single-source catalyst for the metal-catalyzed ROP of the original strained molecule **12**, and the reaction of **29** with an excess of **12** at elevated temperature led to the formation of regioregular poly(troticenylsilanes), in which the Cp–Cht sandwich moieties are exclusively linked *via* Cp–Si–Cht bridges.[8b] In analogy to the metal-catalyzed polymerization of ferrocenophanes such as **14** and **15** (Fig. 7),[48,49] propagation might proceed by sequences of oxidative addition and reductive elimination processes involving the Si–C bonds or *via* σ-bond metathesis of the Pt–Si and Si–C bonds. Reductive elimination from the intermediate platinacyclic oligomers **32** eventually leads to cyclic oligotroticenes **33** (Scheme 9). MALDI-TOF mass spectrometric characterization produced molecular peaks for oligomers **33** between m/z = 1301 (n = 5) and 5985 (n = 23). Unfortunately, the high reactivity of the mixture **33** precluded the isolation and purification of specific oligomers in a similar manner as recently described for dimeric, pentameric and hexameric oligo(ferrocenylsilanes).[50] The calculated structure of a corresponding hexa(troticenylsilane) of type **33** is shown in Scheme 9.

Phosphane-functionalized cycloheptatrienyl–cyclopentadienyl sandwich complexes

In contrast to ferrocenylphosphanes, P-functionalized Cht–Cp sandwich complexes are scarce, and the mono- and diphosphanes $[(\eta^7\text{-}C_7H_6PR_2)Ti(\eta^5\text{-}C_5H_5)]$ (**35**) and $[(\eta^7\text{-}C_7H_6PR_2)Ti(\eta^5\text{-}C_5H_4PR_2)]$ (**34**) (R = Me, Ph) are among the very few examples of functionalized Cht–Cp complexes; they have been obtained by mono- or dilithiation of $[(\eta^7\text{-}C_7H_7)Ti(\eta^5\text{-}C_5H_5)]$ (troticene) followed by reaction with the respective chlorophosphane $ClPR_2$ (Scheme 10). Several transition metal complexes have been synthesized, in which **35** or **34** act as mono- or bidentate phosphane ligands, respectively.[5,6] Taking into account the different reactivities of the Cht–Cp complexes **1**–**3** towards σ-donor/π-acceptor ligands, it could be assumed that related phosphorus-functionalized zirconium and hafnium complexes should feature intermolecular metal–phosphane contacts (*vide supra*).[26] Since the

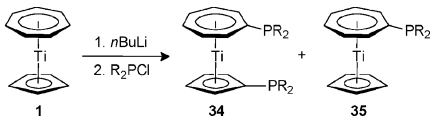

Scheme 10 Preparation of mono- and diphosphanyltroticenes.

lithiation of trozircene (**2**) and trohafcene (**3**) with *n*-BuLi–tmeda in an analogous manner to troticene (**1**) proved unsuccessful, we aimed towards the syntheses of the monophosphane derivatives $[(\eta^7\text{-}C_7H_7)M(\eta^5\text{-}C_5H_4PR_2)]$ (M = Ti, **39**; Zr, **40**; Hf, **41**). The titanium complexes **39** could be obtained from the reduction of $[(\eta^5\text{-}C_5H_4PR_2)TiCl_3]$ (**36**)[51] with magnesium in the presence of cycloheptatriene, whereas the corresponding zirconium and hafnium complexes required the use of the metallocenes $[(\eta^5\text{-}C_5H_4PR_2)_2MCl_2]$ (M = Zr) and **38** (M = Hf)[52] with loss of one Cp ligand (Scheme 11).[53,54]

The molecular structures of **39a**, **39c**, **40a**, **40b** and **41a** could be established by means of X-ray diffraction analyses, and Fig. 14 shows the molecular structures of **39a** and **40a** as representative examples. As expected, no Ti–P contacts could be observed in the solid state for the troticenes **39**, and the Cht and Cp rings remain virtually coplanar. In contrast, the formation of dimeric structures with Zr–P and Hf–P contacts is observed for the trozircenes **40** and trohafcenes **41**. In all cases, the dimerization leads to centrosymmetric metallacycles with a M–P–Ct_5–M–P–Ct_5 sequence (Ct_5 = centroid of the Cp ring; M = Zr, Hf), and the six-membered rings adopt undistorted chair conformations. The metal–phosphorus distances are very long, *e.g.* Zr–P = 2.9833(3) Å in **40b**, indicating weak interactions as expected from the study of the PMe_3 adducts **7** and **11** (*vide supra*).[27] In agreement with the trend of the metal radii,[17] the Zr–P bond of 2.9305(4) Å in **40a** is longer than the Hf–P bond of 2.8034(6) Å in **41a**.

The presence of weak P–Zr and P–Hf bonds in **40** and **41** suggests that these dimers can easily be cleaved and used for the synthesis of transition metal–phosphane complexes, which might exhibit interesting secondary interactions due to the presence of a Lewis acidic Cht–Cp metal site. In fact, any structurally characterized bimetallic complex obtained from the reactions of **40** or **41** features an unusual intramolecular interaction involving the zirconium or hafnium atoms, respectively. Scheme 12 shows two representative examples derived from **40b**. For instance, the reaction with dimeric $[M(\eta^4\text{-}C_8H_{12})Cl]_2$ (C_8H_{12} = 1,5-cyclooctadiene; M = Rh, Ir) furnishes complexes **42** with long Zr–Cl distances of 2.7976(4) Å (M = Rh) and 2.8265(6) Å (M = Ir). A particularly

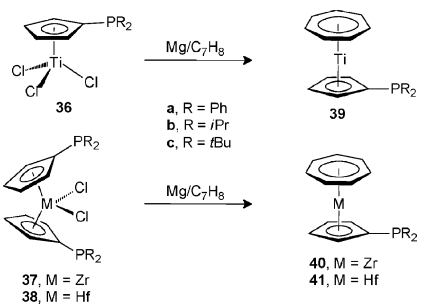

Scheme 11 Preparation of Cp-functionalized Cht–Cp sandwich complexes.

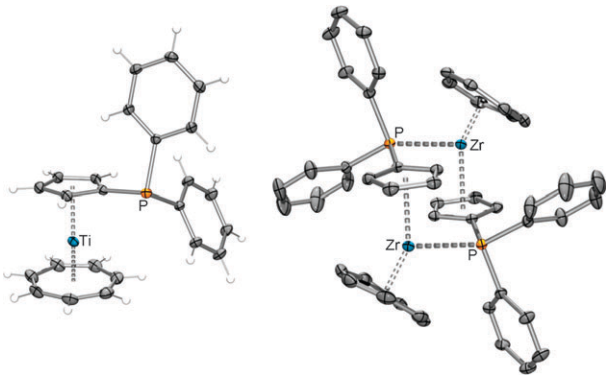

Fig. 14 Molecular structures of **39a** (left) and **40a** (right).

interesting complex can be isolated from the reaction of **40b** with $[Pd(\eta^4\text{-}C_8H_{12})Cl_2]$, which leads to reduction of Pd(II) and formation of the diphosphane–Pd(0) complex **43**. The molecular structure reveals a T-shaped palladium complex with an unprecedented Pd–Zr bond of 2.9709(3) Å (Fig. 15). The angles at palladium are P1–Pd–P2 = 131.83(2)°, P1–Pd–Zr1 = 73.652(11)° and P2–Pd–Zr1 = 152.935(11)°, indicating a strong deviation from a linear arrangement normally observed for dicoordinate structures of the type $[Pd(0)(PR_3)_2]$; for instance P–Pd–P = 180° in $[Pd(FcPtBu_2)_2]$, in which the di-*tert*-butylferrocenylphosphane ligand ($FcPtBu_2$) is incapable of developing a secondary Fe–Pd interaction.[55]

Another selected example for the Lewis acidic behaviour of the Cht–Cp metal sites in complexes **40** and **41** involves the reaction of **40b** with the (dimethylsulfide)chlorogold complex $[(Me_2S)AuCl]$, which did not give the expected 1 : 1 complex [(**40b**)AuCl]. Instead, a 2 : 1 complex of the type $[(\mathbf{40b})_2Au]Cl$ precipitated from solution, irrespective of the applied stoichiometry. The molecular structure in Scheme 13 reveals that this complex contains a cationic diphosphane–gold moiety and that the chloride counterion has been removed from the gold atom and is weakly bound to the two zirconium atoms. The P–Au–P axis is almost linear [172.37(3)°], whereas the Zr–Cl–Zr angle of 135.09(3)° is significantly more acute.

The secondary interactions available in complexes containing the phosphanes **40** and related species will certainly have an impact on the activation of substrates, for instance by oxidative addition to complexes such as **43**. A number of related complexes await their publication,[53] and the full potential of the zirconium– and hafnium–phosphane ligands **40** and **41** as ligands for applications in homogeneous catalysis needs yet to be investigated. Thereby, the Cht–Cp metal

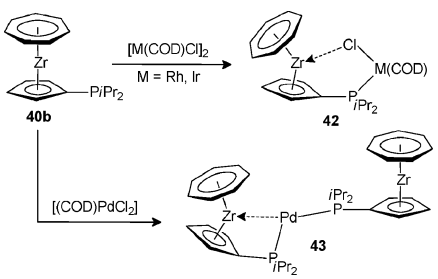

Scheme 12 Synthesis of trozircenylphosphane complexes featuring secondary interactions.

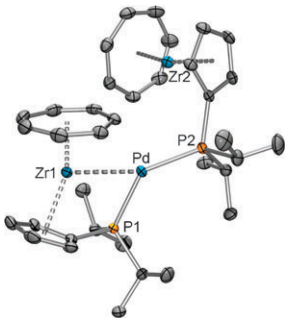

Fig. 15 Molecular structure of the Pd–Zr complex **43**.

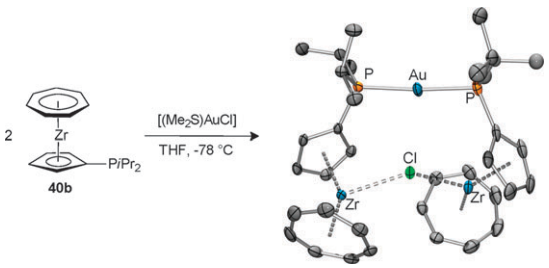

Scheme 13 Synthesis and molecular structure of a bis(trozircenylphosphane)gold complex.

moiety can be regarded as a pendant Lewis acidic acceptor ligand in a similar fashion as described for ambiphilic phosphane ligands featuring pendant borane and alane moieties, which have also been investigated as promising candidates for organotransition metal catalysis, notably *via* intramolecular activation of M–X bonds.[56]

Conclusions and outlook

The detailed experimental and theoretical investigation of 16-electron group 4 Cht–Cp complexes as outlined in this contribution gives clear evidence for a reactivity pattern, which resembles the Lewis acidic behaviour of M^{+IV} complexes (M = Ti, Zr, Hf). For M = Zr and Hf, the metals are accessible without the prerequisite to bridge the two rings. Therefore, functionalized systems such as phosphanyl-substituted trozircenes and trohafcenes of the type $[(\eta^5\text{-}C_5H_4PR_2)M(\eta^7\text{-}C_7H_7)]$ (M = Zr, Hf) are able to exhibit secondary metal–ligand or metal–metal interactions upon coordination to other transition metals (Fig. 16), and the use of these interactions as a steering principle in homogenous catalysis will be further exploited. Isomeric monophosphanes and diphosphanes of the types $[(\eta^5\text{-}C_5H_5)M(\eta^7\text{-}C_7H_6PR_2)]$ and $[(\eta^5\text{-}C_5H_4PR_2)M(\eta^7\text{-}C_7H_6PR_2)]$, respectively, are also interesting alternatives. In addition, the corresponding trotricene derivatives (M = Ti), where secondary interactions involving the titanium atom are absent, represent interesting ligands in their own right, as they might serve as sterically modified analogues of ferrocenylphosphanes.[2]

For Cht–Cp titanium complexes, reactivity at the metal center could be observed only for *ansa*-Cht–Cp complexes. In addition, cleavage of the E–C bond to the seven-membered ring allows the use of these complexes as building blocks for the preparation of metallopolymers. In addition to

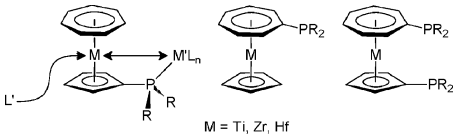

Fig. 16 Secondary interactions in phosphanyl-functionalized Cht–Cp metal complexes.

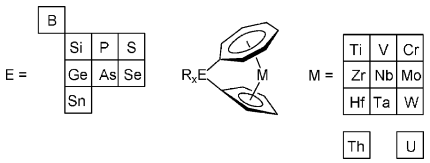

Fig. 17 Variation of *ansa*-cycloheptatrienyl–cyclopentadienyl complexes.

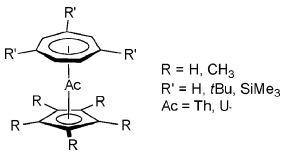

Fig. 18 Cycloheptatrienyl–cyclopentadienyl actinide sandwich complexes.

troticenophanes (M = Ti), *ansa*-Cht–Cp complexes containing vanadium and chromium have been characterized.[8–10] Further development in this area could be achieved by variation of the metal atoms with incorporation of the heavier group 4–6 elements, but could also involve the introduction of other bridging atoms with different atomic radii to fine-tune the reactivity of the resulting complexes (Fig. 17). For R_xE = PR, interaction between the bridging phosphorus atom and the metal atom could be envisaged in the case of titanium, potentially leading to supramolecular aggregation in the solid state.

The heaviest group 4 element is the transactinide rutherfordium; its radioactivity, however, prevents the preparation of organometallic complexes. On the other hand, the high stability of the +4 oxidation state makes thorium an ideal candidate for the preparation of Cht–Cp actinide complexes. In view of the report of the X-ray crystallographic characterization of the bis(cycloheptatrienyl)uranium anion $[(\eta^7\text{-}C_7H_7)_2U]^-$,[57] the preparation of Cht–Cp uranium sandwich complexes as shown in Fig. 18 could also be envisaged. It should be noted that a number of sterically demanding cycloheptatrienyl ligands are also available for this purpose, and the majority of these ligands have been introduced by the author's group.[43,58]

Acknowledgements

This work was supported by the Deutsche Forschungsgemeinschaft through the focus program SPP 1118 "Secondary Interactions as a Steering Principle for the Selective Functionalization of Non-Reactive Substrates". I wish to thank all my co-workers, in particular Dr Andreas Kunst, Dipl.-Chem. Susanne Büschel and Dr Thomas Bannenberg, who have made the most significant contributions to the results presented in this overview.

Notes and references

1. Special Issue: 50th Anniversary of the Discovery of Ferrocene, R. D. Adams, *J. Organomet. Chem.*, 2001, **637–639**, 1.
2. Selected reviews: (*a*) *Ferrocenes*, ed. A Togni and T Hayashi, VCH, Weinheim, 1995; (*b*) G. Bandoli and A. Dolmella, *Coord. Chem. Rev.*, 2000, **209**, 161; (*c*) U. Siemeling and T.-C. Auch, *Chem. Soc. Rev.*, 2005, **34**, 284; (*d*) R. G. Arrayás, J. Adrio and J. C. Carretero, *Angew. Chem., Int. Ed.*, 2006, **45**, 7674; (*e*) K. Osakada, T. Sakano, M. Horie and Y. Suzaki, *Coord. Chem. Rev.*, 2006, **250**, 1012; (*f*) T. J. Colacot, *Chem. Rev.*, 2003, **103**, 3101; (*g*) P. Štěpnička, *Eur. J. Inorg. Chem.*, 2005, 3787; (*h*) R. C. J. Atkinson, V. C. Gibson and N. J. Long, *Chem. Soc. Rev.*, 2004, **33**, 313.
3. Selected reviews: (*a*) *Inorganic and Organometallic Polymers*, ed. V Chandrasekhar, Springer, Heidelberg, 2005; (*b*) P. Nguyen, P. Gomez-Elipe and I. Manners, *Chem. Rev.*, 1999, **99**, 1515; (*c*) *Synthetic Metal Containing Polymers*, ed. I Manner, Wiley-VCH, Weinheim, 2004; (*d*) *Macromolecules Containing Metal and Metal-Like Elements*, ed. A. S. Abd-el-Aziz, C. E. Carraher, Jr, C. U. Pittman, Jr, J. E. Sheats and M Zeldin, Wiley, New York, 2004, vol. 1–3; (*e*) *Inorganic and Organometallic Polymers*, ed. R. D. Archer, Wiley, New York, 2001; (*f*) I. Manners, *Science*, 2001, **294**, 1664; (*g*) D. E. Herbert, U. F. J. Mayer and I. Manners, *Angew. Chem., Int. Ed.*, 2007, **46**, 5060; (*h*) V. Bellas and M. Rehahn, *Angew. Chem., Int. Ed.*, 2007, **46**, 5082.
4. M. L. H. Green and D. K. P. Ng, *Chem. Rev.*, 1995, **95**, 439.
5. (*a*) B. Demerseman and P. H. Dixneuf, *J. Organomet. Chem.*, 1981, **210**, C20; (*b*) B. Demerseman, P. H. Dixneuf, J. Douglade and R. Meicier, *Inorg. Chem.*, 1982, **21**, 3942.
6. (*a*) M. D. Rausch, M. Ogasa, M. A. Ayers, R. D. Rogers and A. N. Rollins, *Organometallics*, 1991, **10**, 2481; (*b*) L. B. Kool, M. Ogasa, M. D. Rausch and R. D. Rogers, *Organometallics*, 1989, **8**, 1785; (*c*) M. Ogasa, M. D. Rausch and R. D. Rogers, *J. Organomet. Chem.*, 1991, **403**, 279.
7. (*a*) C. Elschenbroich, J. Plackmeyer, M. Nowotny, A. Behrendt, K. Harms, J. Pebler and O. Burghaus, *Chem.–Eur. J.*, 2005, **11**, 7427; (*b*) C. Elschenbroich, J. Plackmeyer, M. Nowotny, K. Harms, J. Pebler and O. Burghaus, *Inorg. Chem.*, 2005, **44**, 955; (*c*) C. Elschenbroich, M. Wolf, J. Pebler and K. Harms, *Organometallics*, 2004, **23**, 454; (*d*) C. Elschenbroich, J. Plackmeyer, K. Harms, O. Burghaus and J. Pebler, *Organometallics*, 2003, **22**, 3367; (*e*) C. Elschenbroich, M. Wolf, O. Schiemann, K. Harms, O. Burghaus and J. Pebler, *Organometallics*, 2002, **21**, 5810; (*f*) C. Elschenbroich, F. Lu and K. Harms, *Organometallics*, 2002, **21**, 5152; (*g*) C. Elschenbroich, O. Schiemann, O. Burghaus, K. Harms and J. Pebler, *Organometallics*, 1999, **18**, 3273; (*h*) C. Elschenbroich, M. Wolf, O. Burghaus, K. Harms and J. Pebler, *Eur. J. Inorg. Chem.*, 1999, 2173.
8. (*a*) M. Tamm, A. Kunst, T. Bannenberg, E. Herdtweck, P. Sirsch, C. J. Elsevier and J. M. Ernsting, *Angew. Chem., Int. Ed.*, 2004, **43**, 5530; (*b*) M. Tamm, A. Kunst and E. Herdtweck, *Chem. Commun.*, 2005, 1729; (*c*) M. Tamm, A. Kunst, T. Bannenberg, S. Randoll and P. G. Jones, *Organometallics*, 2007, **26**, 417.
9. C. Elschenbroich, F. Paganelli, M. Nowotny, B. Neumüller and O. Burghaus, *Z. Anorg. Allg. Chem.*, 2004, **630**, 1599.
10. (*a*) H. Braunschweig, M. Lutz and K. Radacki, *Angew. Chem., Int. Ed.*, 2005, **44**, 5647; (*b*) A. Bartole-Scott, H. Braunschweig, T. Kupfer, M. Lutz, I. Manners, T. Nguyen, K. Radacki and F. Seeler, *Chem.–Eur. J.*, 2006, **12**, 1266; (*c*) H. Braunschweig, M. Lutz, K. Radacki, A. Schaumlöffel, F. Seeler and C. Unkelbach, *Organometallics*, 2006, **25**, 4433; (*d*) H. Braunschweig, T. Kupfer, M. Lutz and K. Radacki, *J. Am. Chem. Soc.*, 2007, **129**, 8893.
11. H. O. van Oven and H. J. Liefde Meijer, *J. Organomet. Chem.*, 1970, **23**, 158.
12. H. O. van Oven, C. J. Groenenboom and H. J. Liefde Meijer, *J. Organomet. Chem.*, 1974, **81**, 379.
13. S. Büschel, A. Glöckner and M. Tamm, unpublished results.
14. (*a*) K. A. Lyssenko, M. Y. Antipin and S. Y. Ketkov, *Russ. Chem. Bull.*, 2001, **50**, 130; (*b*) J. D. Zeinstra and J. L. de Boer, *J. Organomet. Chem.*, 1973, **54**, 207.

15. M. Tamm, A. Kunst, T. Bannenberg, E. Herdtweck and R. Schmid, *Organometallics*, 2005, **24**, 3163.
16. For the sandwich compounds [(η^7-C_7H_7)M(η^5-C_5H_5)] (M = Ti, Zr, Hf), we wish to introduce the trivial names troticene,[8a] trozircene and trohafcene, in accord with the naming of [(η-C_7H_7)V(η-C_5H_5)] as trovacene, which stands for [(η^7-*tro*pylium)*va*nadium(η^5-*c*yclop*en*tadi*e*nyl)], see for instance: C. Elschenbroich, O. Schiemann, O. Burghaus and K. Harms, *J. Am. Chem. Soc*., 1997, **119**, 7452. Accordingly, the compound [(η^7-C_7H_7)Cr(η^5-C_5H_5)] has recently been named trochrocene[10].
17. R. D. Shannon, *Acta Crystallogr., Sect. A: Cryst. Phys., Diffr., Theor. Gen. Crystallogr*., 1976, **32**, 751.
18. R. D. Rogers and J. H. Teuben, *J. Organomet. Chem*., 1988, **354**, 169.
19. (*a*) C. J. Groenenboom, H. J. Liefde Meijer and F. Jellinek, *J. Organomet. Chem*., 1974, **69**, 235; (*b*) C. J. Groenenboom, G. Sawatzky, H. J. Liefde Meijer and F. Jellinek, *J. Organomet. Chem*., 1974, **76**, C4.
20. J. D. Zeinstra and W. C. Nieuwpoort, *Inorg. Chim. Acta*, 1978, **30**, 103.
21. D. W. Clack and K. D. Warren, *Theor. Chim. Acta*, 1977, **46**, 313.
22. J. E. Anderson, E. T. Maher and L. B. Kool, *Organometallics*, 1991, **10**, 1248.
23. (*a*) J. C. Green, M. L. H. Green, N. Kaltsoyannis, P. Mountford, P. Scott and S. J. Simpson, *Organometallics*, 1992, **11**, 3353; (*b*) J. C. Green, N. Kaltsoyannis, K. H. Sze and M. MacDonald, *J. Am. Chem. Soc*., 1994, **116**, 1994.
24. (*a*) G. Menconi and N. Kaltsoyannis, *Organometallics*, 2005, **24**, 1189; (*b*) N. Kaltsoyannis, *J. Chem. Soc., Dalton Trans*., 1995, 3727.
25. All DFT calculations have been performed with the Gaussian 03 program suite (M. J. Frisch, G. W. Trucks, H. B. Schlegel, G. E. Scuseria, M. A. Robb, J. R. Cheeseman, J. A. Montgomery, Jr., T. Vreven, K. N. Kudin, J. C. Burant, J. M. Millam, S. S. Iyengar, J. Tomasi, V. Barone, B. Mennucci, M. Cossi, G. Scalmani, N. Rega, G. A. Petersson, H. Nakatsuji, M. Hada, M. Ehara, K. Toyota, R. Fukuda, J. Hasegawa, M. Ishida, T. Nakajima, Y. Honda, O. Kitao, H. Nakai, M. Klene, X. Li, J. E. Knox, H. P. Hratchian, J. B. Cross, V. Bakken, C. Adamo, J. Jaramillo, R. Gomperts, R. E. Stratmann, O. Yazyev, A. J. Austin, R. Cammi, C. Pomelli, J. Ochterski, P. Y. Ayala, K. Morokuma, G. A. Voth, P. Salvador, J. J. Dannenberg, V. G. Zakrzewski, S. Dapprich, A. D. Daniels, M. C. Strain, O. Farkas, D. K. Malick, A. D. Rabuck, K. Raghavachari, J. B. Foresman, J. V. Ortiz, Q. Cui, A. G. Baboul, S. Clifford, J. Cioslowski, B. B. Stefanov, G. Liu, A. Liashenko, P. Piskorz, I. Komaromi, R. L. Martin, D. J. Fox, T. Keith, M. A. Al-Laham, C. Y. Peng, A. Nanayakkara, M. Challacombe, P. M. W. Gill, B. G. Johnson, W. Chen, M. W. Wong, C. Gonzalez and J. A. Pople, *GAUSSIAN 03 (Revision C.02)*, Gaussian, Inc., Wallingford, CT, 2004) using the B3LYP density functional and the 6-311G(d,p) basis set combination for all main group elements. For the transition metal, double zeta basis sets optimized for use with effective core potentials (ECP) in combination with the corresponding Stuttgart ECP were employed (see original publications for further details).
26. (*a*) M. L. H. Green and N. M. Walker, *J. Chem. Soc., Chem. Commun*., 1989, 1865; (*b*) G. M. Diamond, M. L. H. Green, P. Mountford, N. M Walker and J. A. K. Howard, *J. Chem. Soc., Dalton Trans*., 1992, 417.
27. R. J. Baker, T. Bannenberg, A. Kunst, S. Randoll and M. Tamm, *Inorg. Chim. Acta*, 2006, **395**, 4797.
28. K. Wang, G. P. Rosini, S. P. Nolan and A. S. Goldman, *J. Am. Chem.Soc*., 1995, **117**, 5082.
29. T. Brackemeyer, G. Erker and R. Fröhlich, *Organometallics*, 1997, **16**, 531.
30. H. Jacobsen, H. Berke, T. Brackemeyer, T. Eisenblätter, G. Erker, R. Fröhlich, O. Meyer and K. Bergander, *Helv. Chim. Acta*, 1998, **81**, 1692.
31. M. Niehues, G. Kehr, G. Erker, B. Wibbeling, R. Fröhlich, O. Blacque and H. Berke, *J. Organomet. Chem*., 2002, **663**, 192.
32. (*a*) S. K. Ritter, *Chem. Eng. News*, 2007, **85**(41), 42; (*b*) C. Marschner, *Angew. Chem., Int. Ed*., 2007, **46**, 6770; (*c*) Y. Okhi and M. D. Fryzuk, *Angew. Chem., Int. Ed*., 2007, **46**, 3180.
33. Selected examples: (*a*) T. Beweries, V. V. Burlakov, M. A. Bach, S. Peitz, P. Arndt, W. Baumann, A. Spannenberg, U. Rosenthal, B. Pathak and E. D. Jemmis, *Angew. Chem., Int. Ed*., 2007, **46**, 6907; (*b*) W. H. Bernskoetter, E. Lobkovsky and P. J. Chirik, *Angew. Chem., Int. Ed*., 2007, **46**, 2858; (*c*) T. Beweries, V. V. Burlakov, M. A. Bach, P. Arndt, W. Baumann, A. Spannenberg and U. Rosenthal, *Organometallics*, 2007, **26**, 247.
34. W. Finckh, B.-Z. Tang, D. A. Foucher, D. B. Zamble, R. Ziembinski, A. Lough and I. Manners, *Organometallics*, 1993, **12**, 823.
35. D. A. Foucher, M. Edwards, R. A. Burrow, A. J. Lough and I. Manners, *Organometallics*, 1994, **13**, 4959.
36. K. Hultzsch, J. M. Nelson, A. J. Lough and I. Manners, *Organometallics*, 1995, **14**, 5496.
37. C. Elschenbroich, E. Schmidt, R. Gondrum, B. Metz, O. Burghaus, W. Massa and S. Wocadlo, *Organometallics*, 1997, **16**, 4589.
38. M. Elian, M. M. L. Chen, D. M. P. Mingos and R. Hoffmann, *Inorg. Chem*., 1976, **15**, 1148.
39. D. Gourier and D. Samuel, *Inorg. Chem*., 1988, **27**, 3018.
40. R. Rulkens, D. P. Gates, D. Balaishis, J. K. Pudelski, D. F. McIntosh, A. J. Lough and I. Manners, *J. Am. Chem. Soc*., 1997, **119**, 10976.
41. L. Fielding, *Tetrahedron*, 2000, **56**, 6151.
42. H. A. Benesi and J. H. Hildebrand, *J. Am. Chem. Soc*., 1949, **71**, 2703.
43. M. Tamm, B. Dreßel, R. Fröhlich and K. Bergander, *Chem. Commun*., 2000, 1731.
44. J. Li and B. E. Bursten, *J. Am. Chem. Soc*., 1997, **119**, 9021.
45. D. A. Foucher, B. Z. Tang and I. Manners, *J. Am. Chem. Soc*., 1992, **114**, 6246.
46. J. C. Green, *Chem. Soc. Rev*., 1998, **27**, 263.
47. S. C. Bourke, M. J. MacLachlan, A. J. Lough and I. Manners, *Chem.–Eur. J*., 2005, **11**, 1989.
48. (*a*) J. B. Sheridan, A. J. Lough and I. Manners, *Organometallics*, 1996, **15**, 2195; (*b*) N. P. Reddy, N. Choi, S. Shimada and M. Tanaka, *Chem. Lett*., 1996, 649; (*c*) J. B. Sheridan, K. Temple, A. J. Lough and I. Manners, *J. Chem. Soc., Dalton Trans*., 1997, 711.
49. (*a*) K. Temple, A. J. Lough, J. B. Sheridan and I. Manners, *J. Chem. Soc., Dalton Trans*., 1998, 2799; (*b*) K. Temple, F. Jäkle, J. B. Sheridan and I. Manners, *J. Am. Chem. Soc*., 2001, **123**, 1355; (*c*) W. Y. Chan, A. Berenbaum, S. B. Clendenning, A. J. Lough and I. Manners, *Organometallics*, 2003, **22**, 3796.
50. W. Y. Chan, A. J. Lough and I. Manners, *Angew. Chem., Int. Ed*., 2007, **46**, 9069.
51. J. C. Flores, R. Hernandez, P. Royo, A. Butt, T. P. Spaniol and J. Okuda, *J. Organomet. Chem*., 2000, **593–594**, 202.
52. C. Cornelissen, G. Erker, G. Kehr and R. Fröhlich, *Organometallics*, 2005, **24**, 214.
53. S. Büschel, A.-K. Jungton, C. Hrib and M. Tamm, unpublished results.
54. M. Tamm and S. Büschel, *Polym. Prepr. (Am. Chem. Soc., Div. Polym. Chem.)*, 2007, **48**, 669.
55. G. Mann, C. Incarvito, A. L. Rheingold and J. F. Hartwig, *J. Am. Chem. Soc*., 1999, **121**, 3224.
56. For selected recent examples, see: (*a*) M. Sircoglou, S. Bontemps, M. Mercy, N. Saffon, M. Takahashi, G. Bouhadir, L. Maron and D. Bourissou, *Angew. Chem., Int. Ed*., 2007, **46**, 8583; (*b*) S. Bontemps, G. Bouhadir, K. Miqueu and D. Bourissou, *J. Am. Chem. Soc*., 2006, **128**, 12056.
57. T. Arliguie, M. Lance, M. Nierlich, J. Vigner and M. Ephritikhine, *J. Chem. Soc., Chem. Commun*., 1995, 183.
58. (*a*) M. Tamm, B. Dreßel, R. Fröhlich and K. Bergander, *Chem. Commun*., 2000, 1731; (*b*) M. Tamm, B. Dreßel and R. Fröhlich, *J. Org. Chem*., 2000, **65**, 6795; (*c*) M. Tamm, T. Bannenberg, B. Dreßel, R. Fröhlich and D. Kunz, *Organometallics*, 2001, **20**, 900; (*d*) M. Tamm, K. Baum, R. Fröhlich and Pauli Saarenketo, *Organometallics*, 2001, **20**, 1376; (*e*) M. Tamm, T. Bannenberg, R. Fröhlich, S. Grimme and M. Gerenkamp, *Dalton Trans*., 2004, 482.

